AFRL-RX-WP-TP-2009-4356

A MODEL FOR THE OXIDATION OF ZrB_2, HfB_2 AND TiB_2 (POSTPRINT)

T.A. Parthasarathy, R.A. Rapp, M. Opeka, and R.J. Kerans

Ceramics Branch
Metals, Ceramics, and NDE Division

MARCH 2007

AIR FORCE RESEARCH LABORATORY
MATERIALS AND MANUFACTURING DIRECTORATE
WRIGHT-PATTERSON AIR FORCE BASE, OH 45433-7750
AIR FORCE MATERIEL COMMAND
UNITED STATES AIR FORCE

NOTICE AND SIGNATURE PAGE

Using Government drawings, specifications, or other data included in this document for any purpose other than Government procurement does not in any way obligate the U.S. Government. The fact that the Government formulated or supplied the drawings, specifications, or other data does not license the holder or any other person or corporation; or convey any rights or permission to manufacture, use, or sell any patented invention that may relate to them.

This report was cleared for public release by the USAF 88th Air Base Wing (88 ABW) Public Affairs Office (PAO) on 20 May 2009 and is available to the general public, including foreign nationals. Copies may be obtained from the Defense Technical Information Center (DTIC) (http://www.dtic.mil).

AFRL-RX-WP-TP-2009-4356 HAS BEEN REVIEWED AND IS APPROVED FOR PUBLICATION IN ACCORDANCE WITH THE ASSIGNED DISTRIBUTION STATEMENT.

*//Signature//

KENNETH DAVIDSON, Project Engineer
Metals Branch
Metals, Ceramics, & NDE Division
Nonmetallic Materials Division

//Signature//

MICHAEL J. KINSELLA, Chief
Ceramics Branch
Metals, Ceramics, & NDE Division

//Signature//

ROBERT MARSHALL, Asst Division Chief
Metals, Ceramics, & NDE Division
Materials and Manufacturing Directorate

This report is published in the interest of scientific and technical information exchange, and its publication does not constitute the Government's approval or disapproval of its ideas or findings.

*Disseminated copies will show "//Signature//" stamped or typed above the signature blocks.

REPORT DOCUMENTATION PAGE

Form Approved
OMB No. 0704-0188

1. REPORT DATE *(DD-MM-YY)*	2. REPORT TYPE	3. DATES COVERED *(From - To)*
March 2007	Journal Article Postprint	01 December 2006 – 01 March 2007

4. TITLE AND SUBTITLE
A MODEL FOR THE OXIDATION OF ZrB_2, HfB_2 AND TiB_2 (POSTPRINT)

5a. CONTRACT NUMBER
In-house

5b. GRANT NUMBER

5c. PROGRAM ELEMENT NUMBER
62102F

6. AUTHOR(S)
T.A. Parthasarathy (UES, Inc.)
R.A. Rapp (The Ohio State University)
M. Opeka (Naval Surface Warfare Center)
R.J. Kerans (AFRL/RXLN)

5d. PROJECT NUMBER
5220

5e. TASK NUMBER
00

5f. WORK UNIT NUMBER
52200002

7. PERFORMING ORGANIZATION NAME(S) AND ADDRESS(ES)
UES, Inc.
Dayton, OH 45432

The Ohio State University
Columbus, OH

Naval Surface Warfare Center
West Bethesda, MD

Ceramics Branch (AFRL/RXLN)
Metals, Ceramics, and NDE Division
Materials and Manufacturing Directorate
Wright-Patterson Air Force Base, OH 45433-7750
Air Force Materiel Command, United States Air Force

8. PERFORMING ORGANIZATION REPORT NUMBER
AFRL-RX-WP-TP-2009-4356

9. SPONSORING/MONITORING AGENCY NAME(S) AND ADDRESS(ES)
Air Force Research Laboratory
Materials and Manufacturing Directorate
Wright-Patterson Air Force Base, OH 45433-7750
Air Force Materiel Command
United States Air Force

10. SPONSORING/MONITORING AGENCY ACRONYM(S)
AFRL/RXLN

11. SPONSORING/MONITORING AGENCY REPORT NUMBER(S)
AFRL-RX-WP-TP-2009-4356

12. DISTRIBUTION/AVAILABILITY STATEMENT
Approved for public release; distribution unlimited.

13. SUPPLEMENTARY NOTES
Journal article published in *Acta Materialia*, V. 55 (2007). PAO Case Number: 88ABW-2009-2153; Clearance Date: 20 May 2009. Paper contains color.

14. ABSTRACT
A mechanistic model that interprets the oxidation behavior of the diborides of Zr, Hf and Ti in the temperature range of ~1000–1800 °C was formulated. Available thermodynamic data and literature data for vapor pressures and diffusivities were used to evaluate the model. Good correspondence was obtained between theory and experiments for weight gain, recession and scale thickness as functions of temperature and oxygen partial pressure. At temperatures below about 1400 °C, the rate-limiting step is the diffusion of dissolved oxygen through a film of liquid boria in capillaries at the base of the oxidation product. At higher temperatures, the boria is lost by evaporation, and the oxidation rate is limited by Knudsen diffusion of molecular oxygen through the capillaries between nearly columnar blocks of the oxide, MO_2.

15. SUBJECT TERMS
model, oxidation, ZrB_2, HfB_2, TiB_2

16. SECURITY CLASSIFICATION OF:			17. LIMITATION OF ABSTRACT:	18. NUMBER OF PAGES	19a. NAME OF RESPONSIBLE PERSON (Monitor)
a. REPORT	b. ABSTRACT	c. THIS PAGE			Kenneth E. Davidson
Unclassified	Unclassified	Unclassified	SAR	18	19b. TELEPHONE NUMBER *(Include Area Code)* N/A

Standard Form 298 (Rev. 8-98)
Prescribed by ANSI Std. Z39-18

Available online at www.sciencedirect.com
ScienceDirect
Acta Materialia 55 (2007) 5999–6010
Acta MATERIALIA
www.elsevier.com/locate/actamat

A model for the oxidation of ZrB_2, HfB_2 and TiB_2

T.A. Parthasarathy [a,*], R.A. Rapp [b], M. Opeka [c], R.J. Kerans [d]

[a] UES, Inc., Dayton, OH 45432, USA
[b] The Ohio State University, Columbus, OH, USA
[c] Naval Surface Warfare Center, Carderock Division, West Bethesda, MD, USA
[d] Air Force Research Laboratory, Materials and Manufacturing Directorate, AFRL/MLLN, Wright-Patterson AFB, OH 45433-7817, USA

Received 16 March 2007; accepted 7 July 2007
Available online 4 September 2007

Abstract

A mechanistic model that interprets the oxidation behavior of the diborides of Zr, Hf and Ti in the temperature range of ~1000–1800 °C was formulated. Available thermodynamic data and literature data for vapor pressures and diffusivities were used to evaluate the model. Good correspondence was obtained between theory and experiments for weight gain, recession and scale thickness as functions of temperature and oxygen partial pressure. At temperatures below about 1400 °C, the rate-limiting step is the diffusion of dissolved oxygen through a film of liquid boria in capillaries at the base of the oxidation product. At higher temperatures, the boria is lost by evaporation, and the oxidation rate is limited by Knudsen diffusion of molecular oxygen through the capillaries between nearly columnar blocks of the oxide, MO_2.

Keywords: Model; Oxidation; ZrB_2; HfB_2; TiB_2

1. Introduction

Components in high-flow environments, such as the leading edge of a hypersonic vehicle, are subjected to very high temperatures and require that the geometric integrity be maintained during service [1,2]. The high temperatures and the low-pressure environment make oxidation and evaporative loss critical factors in material selection [3]. The diborides of Zr and Hf, which are termed ultra-high-temperature ceramics (UHTCs), have high melting points and are among the most promising materials for long-term service under hypersonic conditions [3,4]. The diborides are also attractive due to their high thermal conductivity, which is useful to offset the stringent thermal gradients imposed by aerothermal heating. These diborides have also been considered as coatings for protection of carbon-based composites [5] and titanium alloys [6].

A history of studies on the oxidation of diborides is given by Opeka et al. [3]. Based on the promise shown from early works, a good oxidation screening study of the refractory diborides of Ti, Zr, Hf, Nb and Ta was conducted by Kaufman et al. [7,8] and later summarized by Fenter [9]. They reported that the diborides of Zr and Hf are the most oxidation resistant. They further reported that additions of SiC up to 20% by volume further improved the oxidation resistance of these materials. Opeka et al. [3,4,10] pointed out that the high melting points and low vapor pressures of the oxides and sub-oxides of Zr and Hf, and the beneficial vapor pressure vs. P_{O_2} relationships for BO_x species, are responsible for the superior high-temperature resistance of these materials. Using volatility diagrams, they further showed that the diborides of Zr and Hf appear to have the least problem with respect to disruption of the product scale by vapor species. Zr and Hf carbides are limited by CO partial pressures that exceed 1 atm above 1730 °C, yielding a porous and non-protective oxide scale. Silica has very low diffusivities for oxygen and is a very protective scale at more moderate temperatures, but active oxidation to gaseous SiO

* Corresponding author.
E-mail address: Triplicane.parthasarathy@wpafb.af.mil (T.A. Parthasarathy).

1359-6454/$30.00
doi:10.1016/j.actamat.2007.07.027

disrupts the scale above approximately 1800 °C [3,4,10]. Consequently, SiC, Si_3N_4 and transition metal silicides are not very useful at ultra-high temperatures. In contrast, boric oxide is glassy, flows to fill pores in the oxide scale and exhibits a 1 atm partial pressure (for gaseous B_2O_3) only at 1950 °C, despite its well-known tendency to evaporate at moderate temperatures (above ~1200 °C). The gaseous B_2O_3 evaporates at open surface sites without disrupting the scale. When SiC is added to the system, further improvements are realized since the silica-based glass offers greater resistance to evaporation than B_2O_3 alone [11].

Thus far, the understanding of the superior oxidation behavior of the diborides has been primarily qualitative. For engineering design and applications, a quantitative model is needed that predicts all aspects of oxidation. It is desirable to predict factors such as scale thickness, substrate recession and weight change, under a set of complex conditions of temperature and environment. Many experimental works have been conducted under isothermal conditions and in a laboratory environment, while real engineering conditions involve thermal gradients, environmental gradients and turbulent gas flow.

The long-term objective of this work is to develop a model that can be applied to aid engineering design for hypersonic environments. However, the complex nature of the materials makes it necessary to start with a model for simpler systems and conditions, where reliable and well-defined experimental data are available. In this paper, we present a model that is found to predict the scale thickness, metal recession and weight changes for the oxidation of Zr, Hf and Ti diborides under isothermal and slow gas flow conditions. Various factors such as residual boria content and dependencies on temperature and oxygen partial pressure are also predicted and found to be in reasonable agreement with experiments. This model provides a reasonable basis for future work.

2. Conceptual framework

The model reported in this work is based on concepts of the oxidation process derived from microstructural details available in the literature. The morphology of the oxidation product, as well as the phases present and their distribution, has been reported by several researchers [3,4,9,10,12]. For ZrB_2 (or HfB_2), oxidation in air results in a dense adherent oxide scale consisting of two phases, ZrO_2 (or HfO_2) and B_2O_3. No intermediate phases or borates of these systems are observed at the interfaces. The distribution of the phases in the scale varies with temperature. At lower temperatures ($\lesssim$1000 °C), a glassy B_2O_3 film is observed on top of the ($ZrO_2 + B_2O_3$) scale, but this external boria layer is absent at higher temperatures. At all temperatures a porous zirconia scale is one component of the oxidation product. At low and intermediate temperatures, the pores in the zirconia are filled with boria. Further, the microstructure of the ZrO_2 appears to change from equiaxed grains at temperatures below ~1000 °C, to columnar grains at higher temperatures. At higher temperatures, the outer surface of the scale is nodular ZrO_2, and the cross-section reveals a columnar structure of ZrO_2 with a glassy B_2O_3 in between the columnar grains. A similar transition in oxidation rates has been noted with respect to oxygen partial pressure. The dependence of the oxidation rate on the oxygen partial pressure changes from linear to no dependence as the temperature is increased above 1150 °C for ZrB_2 [13]. In addition to these two experimentally observed temperature regimes, it is expected that a high-temperature regime exists where there is very little or no boria in the scale. The three regimes are shown schematically in Fig. 1. In this work, we focus on the intermediate temperature regime, which is the regime of engineering interest. The model developed here predicts the temperature range of

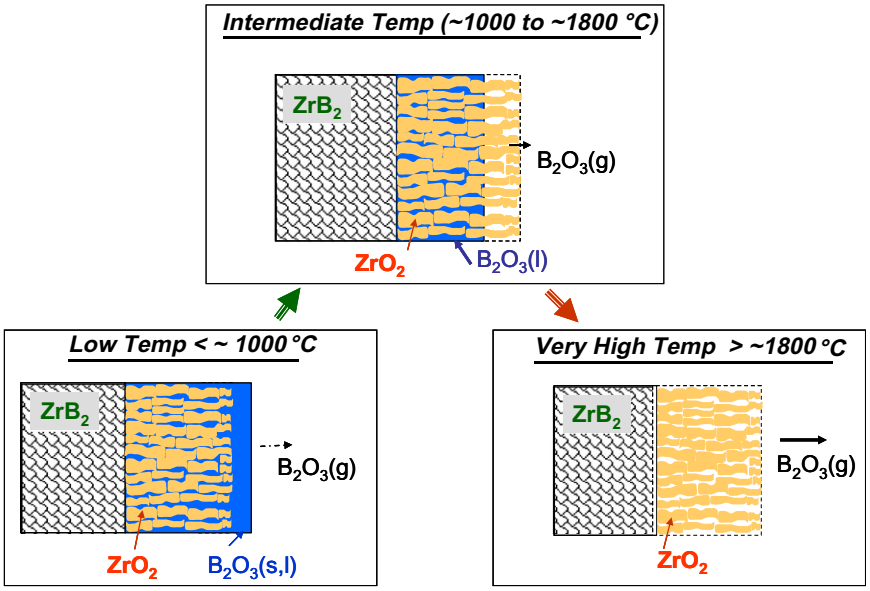

Fig. 1. The oxidation products formed during oxidation of ZrB_2 in three temperature regimes.

the intermediate regime and the oxidation behavior within this intermediate regime.

The conceptual framework for the oxidation in the intermediate temperature regime is shown schematically in Fig. 2a, and the steps considered in the model are shown in Fig. 2b. For oxidation at intermediate temperatures, oxidation of the metal (in the diboride) results in an evaporation-resistant refractory oxide that forms a porous skeleton. The oxidation of the boron results in a glassy boric oxide that flows to fill the base of the porous skeleton. At the surface, the boria evaporates. Both oxidation reactions occur at the refractory substrate–scale interface by the inward diffusion of oxidant species. At steady state, oxidation takes place by both gaseous diffusion of oxygen through the open pores in the oxide skeleton, and by dissolved oxygen diffusing through the liquid boria (at the base of the porous skeleton beneath the surface) to reach the ZrB_2–scale interface. The two reactions are:

$$ZrB_2 + \frac{5}{2}O_2 \rightarrow ZrO_2 + B_2O_3 \quad (1)$$

$$B_2O_3\ (l) \rightarrow B_2O_3\ (g) \quad (2)$$

The rate of dissolution of oxygen into B_2O_3 is not taken to be rate limiting in the model developed below. The transport of oxygen through the refractory oxide is assumed to be negligible compared to that through the pores filled with glassy boria. At temperatures of interest (above 1000 K), B_2O_3 (v) has been shown to be the dominant vapor species at oxygen partial pressures greater than that in equilibrium with ZrB_2 and ZrO_2 [12].

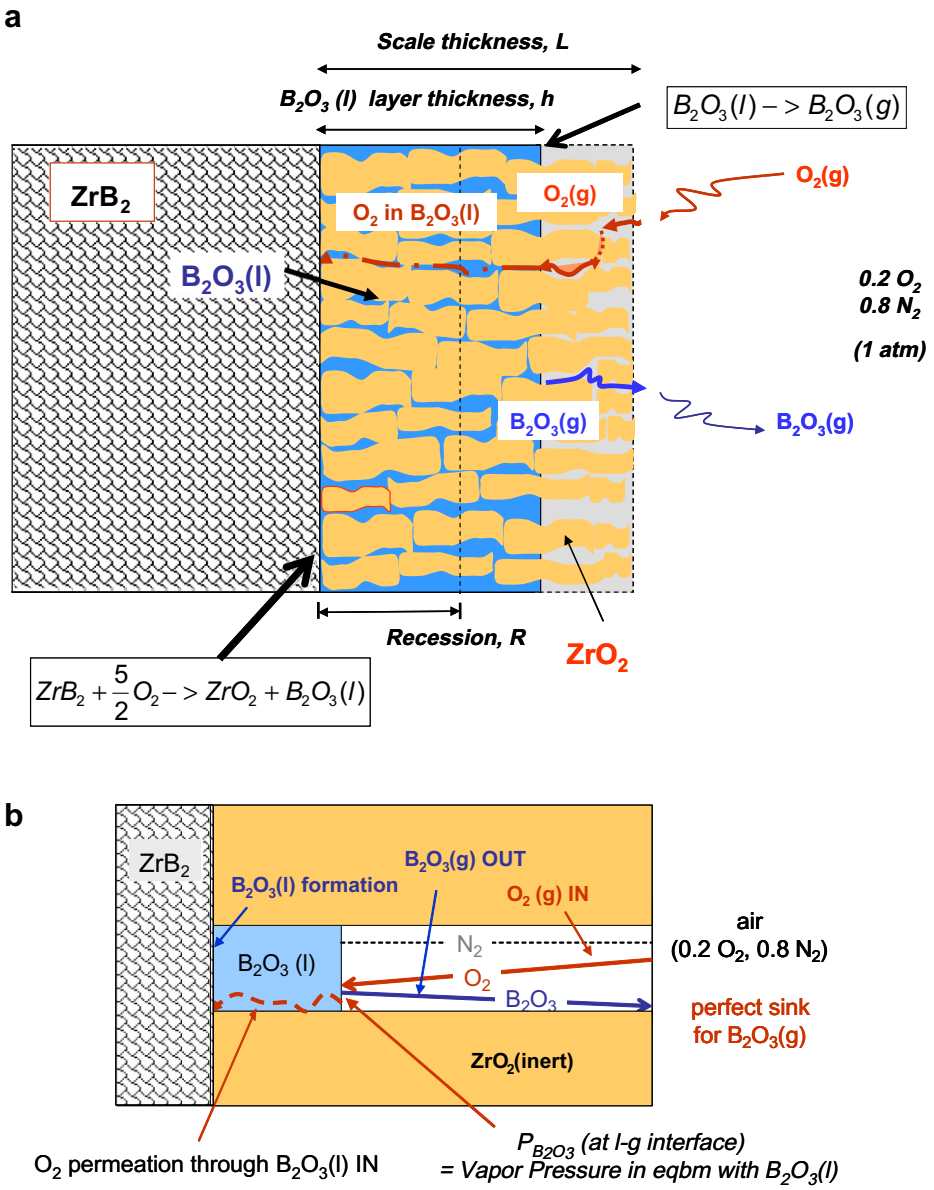

Fig. 2. (a) Schematic sketch of mechanisms involved oxidation of ZrB_2 in air, in the intermediate temperature regime (1000–1800 °C). (b) Schematic of the mechanistic steps considered in the model.

3. The model

The objective of the model is to predict the kinetics of scale thickness, substrate recession and weight change as a function of time at temperature and oxygen partial pressure. A schematic for the model is shown in Fig. 2b. Dense ZrO_2 is assumed to be a barrier to oxygen permeation, due to its negligible rate of ambipolar diffusion. The validity of this assumption is presented in the Appendix. The porosity between ZrO_2 columns is assumed to be continuous, and tortuosity is neglected.

The ambient air is taken to consist of N_2 and O_2 only. A fraction, f, of the scale is taken to be porous and provide a continuous pathway for gaseous diffusion and for the evaporation of liquid B_2O_3 at the surface, which is taken to be a perfect sink for B_2O_3. The relative rates of filling the pore by oxidation at the substrate–scale interface and the evaporation of B_2O_3 determines the extent to which the pores are filled with B_2O_3. At a given time, t, the total scale has a thickness of L and its inner portion is filled with liquid B_2O_3 to a thickness, h. The distance L–h is the diffusion distance in the pore over which gaseous oxygen must diffuse to reach the B_2O_3. The oxygen is assumed to dissolve in B_2O_3 and continue to diffuse to the substrate–scale interface where the oxidation reaction occurs. As explained in the Appendix, the dense zirconia columns are considered to be impervious to oxygen.

At the substrate–scale interface, reaction (1) takes place. Thus, at steady state, the diffusional flux of oxygen must be balanced by the formation rates of ZrO_2 and B_2O_3.

$$|J_{O_2}| = \frac{5}{2}\dot{n}_{B_2O_3} = \frac{5}{2}\dot{n}_{ZrO_2}. \tag{3}$$

The flux of gaseous oxygen in the porous channel that is L–h long is given by:

$$|J_{O_2}| = fD_{O_2}\frac{C^a_{O_2} - C^i_{O_2}}{L-h}, \tag{4}$$

where D is the diffusion coefficient, C the concentration, the superscript "i" refers to the interface between B_2O_3 (l) and the gas phase, which is at a distance h from the substrate–scale interface, and the superscript "a" refers to the scale–ambient interface. Similarly, the flux of B_2O_3 (v) from the surface of B_2O_3 (l) to the ambient, is given by:

$$J_{B_2O_3} = fD_{B_2O_3}\frac{C^i_{B_2O_3} - C^a_{B_2O_3}}{L-h}. \tag{5}$$

Taking $J_{B_2O_3} = n_{B_2O_3}$ (quasi-steady state), and combining Eqs. (3)–(5) the concentration of molecular oxygen at the B_2O_3 liquid–vapor interface is obtained as:

$$C^i_{O_2} = C^a_{O_2} - \frac{5}{2}\frac{D_{B_2O_3}}{D_{O_2}}(C^i_{B_2O_3} - C^a_{B_2O_3}). \tag{6}$$

The concentration $C^a_{B_2O_3}$ at the ambient surface is taken to be zero. The concentration $C^i_{B_2O_3}$ of the B_2O_3 (v) at this interface, which does not depend on the local oxygen pressure, is obtained from vapor pressure data [14]:

$$C^i_{B_2O_3} = \frac{P_{B_2O_3}}{RT}; \quad P_{B_2O_3}\ (\text{atm}) = 3\times 10^8 \exp\left(-\frac{45,686}{T}\right). \tag{7}$$

The permeability of oxygen through the liquid B_2O_3 depends on the oxygen activity gradient across the liquid layer of thickness t. From the ideal gas law, the oxygen partial pressure at the B_2O_3 liquid–vapor interface is given by,

$$P^i_{O_2} = RTC^i_{O_2}. \tag{8}$$

The activity of oxygen at the scale–B_2O_3 interface is given by:

$$K_{\text{reaction1}} = \frac{a_{ZrB_2}(P^s_{O_2})^{5/2}}{a_{B_2O_3}a_{ZrO_2}}. \tag{9}$$

Using the thermodynamic data of Barin [14] for reaction (1), and equating the activities of the solid phases to unity, Eq. (9) gives the following for the oxygen activity, $P^s_{O_2}$, at the substrate ZrB_2–B_2O_3 interface (s):

$$P^s_{O_2}\ (\text{atm}) = 5\times 10^{10}\exp\left(-\frac{99,967}{T}\right). \tag{10}$$

The values given by Eq. (10) are consistent with the maps presented by Fahrenholtz [12]. The diffusivity of oxygen through boria has been measured by Tokuda et al. [15], who found a linear dependence of the permeation flux on oxygen partial pressure and deduced that molecular oxygen diffuses. The oxygen flux across the liquid boria, $J_{O_2}(B_2O_3)$, is related to the partial pressure gradient through the oxygen permeability coefficient, Π, as [16,17]:

$$|J_{O_2}(B_2O_3)| = \frac{\Pi_{O_2-B_2O_3}}{h} f\left[P^i_{O_2} - P^s_{O_2}\right]. \tag{11}$$

The oxygen permeability coefficient, $\Pi_{O_2-B_2O_3}$, is obtained from the literature [15,17] as:

$$\Pi_{O_2-B_2O_3}\ (\text{mol/m s atm}) = 0.15\exp\left(\frac{-16,000}{T}\right). \tag{12}$$

Substituting Eq. (12) into Eq. (11) and equating the flux of oxygen through the gaseous layer, given by Eq. (4), an equation relating the boria layer thickness, h, to the scale thickness, L, is obtained:

$$h = qL; \quad q = \frac{\Pi_{O_2-B_2O_3}(P^i_{O_2} - P^s_{O_2})}{D_{O_2}(C^a_{O_2} - C^i_{O_2}) + \Pi_{O_2-B_2O_3}(P^i_{O_2} - P^s_{O_2})}. \tag{13}$$

The equations for the rate of change of scale thickness (L) and mass (W) of the scale are given by accounting for the flux balance using Eq. (3)

$$\frac{dL}{dt} = \left(\frac{1}{1-f}\right)\left(\frac{1}{\rho_{ZrO_2}}\right)\frac{dW_{ZrO_2}}{dt} = \left(\frac{1}{1-f}\right)\frac{2}{5}J_{O_2}\frac{M_{ZrO_2}}{\rho_{ZrO_2}}, \tag{14}$$

where ρ refers to density and M to molar volume. Combining with Eq. (4), one obtains:

$$\frac{dL}{dt} = \frac{2}{5}\left(\frac{M_{ZrO_2}}{\rho_{ZrO_2}}\right)\left(\frac{f}{1-f}\right)D_{O_2}\frac{C^a_{O_2} - C^i_{O_2}}{L(1-q)}. \quad (15)$$

Integration of Eq. (15) gives a parabolic equation for growth of the scale:

$$L^2 = 2\left[\frac{2}{5}\left(\frac{M_{ZrO_2}}{\rho_{ZrO_2}}\right)\left(\frac{f}{1-f}\right)D_{O_2}\frac{C^a_{O_2} - C^i_{O_2}}{(1-q)}\right]t. \quad (16)$$

The magnitude of recession of the substrate is given by:

$$R = L(1-f)\frac{M_{ZrB_2}/\rho_{ZrB_2}}{M_{ZrO_2}/\rho_{ZrO_2}}. \quad (17)$$

The total weight change per unit area is given by:

$$\frac{\Delta W}{A} = L\rho_{ZrO_2}(1-f) + hf\rho_{B_2O_3} - R\rho_{ZrB_2}. \quad (18)$$

It remains to evaluate the diffusion coefficient of gaseous oxygen through the porous region filled with oxygen, B_2O_3 (g) and nitrogen. The diffusion coefficient in a multi-component gaseous system can be approximated by [18]:

$$D_{1,(2,\ldots,i)} = \frac{1}{\sum_i^{i\neq 1}(x_i/D_{1-i})}; \quad x_i = \frac{n_i}{\sum_j^{j\neq 1} n_j}, \quad (19)$$

where D refers to diffusivity, n to mole fraction, subscript "1, (2, ..., i)" refers to the diffusivity of species 1 in a medium of i species, subscript "$1-i$" refers to the diffusivity of species 1 in a binary mixture of species 1 and i. The diffusivity D_{1-2} of species 1 in a binary gas mixture with species 2 is given by [19]:

$$D_{1-2} = \frac{0.0018583T^{3/2}\sqrt{(1/M_1)+(1/M_2)}}{r_{12}^2\Omega_D P} \quad (20)$$

where D_{1-2} is the gas diffusivity in cm^2/s;

$$\Omega_D = \frac{1.06036}{T^{*0.15610}} + \frac{0.193000}{\exp(0.47635T^*)} + \frac{1.03587}{\exp(1.52996T^*)} + \frac{1.76474}{\exp(3.89411T^*)},$$

$T^* = \frac{kT}{\varepsilon_{12}}$, $\varepsilon_{12} = \sqrt{\varepsilon_1\varepsilon_2}$, $r_{12} = 0.5(r_1 + r_2)$ in Å, P = pressure in atm; M_i = molecular weight (g/mol).

The parameters needed for the above expressions can be obtained from the work of Svehla [20]. When the size of the pore is small, the mean free path is longer than the characteristic dimension of the system, and the diffusion of gases is governed by Knudsen diffusion [21]:

$$D_k = \frac{4}{3}\left(\frac{8RT}{\pi M}\right)^{1/2}\frac{r}{2}, \quad (21)$$

where D_k is the Knudsen diffusivity, M the molecular mass of the diffusing species and r the radius of the porous pathway. The effective diffusivity is given by [21]:

$$D_{eff} = (D_k^{-1} + D_{1-2}^{-1})^{-1}. \quad (22)$$

Using Eqs. (19)–(22), Eqs. (16)–(18) give the scale thickness, recession and weight gain as a function of temperature, time and partial pressure of oxygen.

4. Model predictions compared with literature data

4.1. ZrB_2

The model was verified by comparing its predictions with experimental data reported in the literature for the oxidation of ZrB_2. As can be seen from the development in Section 3, most of the parameters needed for the prediction can be obtained from the literature. Two parameters in the model that are not well known are the pore fraction and pore radius, and they are likely to vary between experiments depending on starting microstructure and oxidation conditions such as temperature and environment. The values of 0.05 and 0.5 μm, respectively, were chosen to get the best fit with all of the experimental data for ZrB_2, but were kept the same for HfB_2 and TiB_2. From what can be inferred from micrographs of oxide scales presented in the literature, these values are quite plausible. The sensitivity of the predictions to the choice of these variables was examined and is presented in a later section. The other significant unknowns are the velocities and water contents of the atmospheres in the experiments. Future experimenters are encouraged to report these parameters; they can have large effects.

Extensive thermogravimetric analysis (TGA) data on weight change vs. time in 250 Torr of pure oxygen was reported by Tripp and Graham [22]. They compared their results with the parabolic rate constant data from Berko-

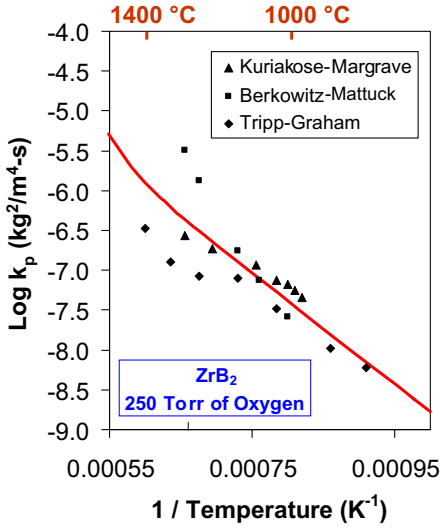

Fig. 3. The experimental data from three different works in the literature [12,22,23] on the parabolic rate constant of measured weight gain of samples in 250 Torr of pure oxygen at different temperatures are shown compared with the model predictions. The porosity in the scale, f, was taken to be 0.05 and the pore radius to be 0.5 μm.

witz-Mattuck [13] and Kuriakose and Margrave [23]. Fig. 3 shows the results from all three experimental works, compared with the model predictions, for an assumed pore fraction of 0.05 and pore radius of 0.5 μm. The weight gain data of Tripp and Graham are lower than the model predictions at temperatures above 1200 °C. The lower values of experimental data could arise from a low gas flow rate used in the experiment, while the model assumes a perfect sink for B_2O_3 (v). However, when the model is compared with all of the reported data, the correspondence is taken to be good in that it matches well at low temperatures and is a good representation of the widely scattered data at high temperatures.

Fenter summarized the metal recession of several diborides in air, as a function of temperature [9]. The results for ZrB_2 in Fig. 4a are compared to the model prediction. The model compares very well with data up to ~1850 °C, above which the model predicts that the high-temperature regime dominates and that all of the boria will evaporate as soon as it forms. The experimental data show a significant enhancement in recession at this temperature. The model predicts the transition temperature correctly. The reason for the upward trend in recession is not clear; one possibility is significant spallation of MO_2 due to the absence of boria at higher temperature.

Finally, Opeka et al. [3,10] and Talmy et al. [24] have reported the mass change and oxide layer thicknesses of ZrB_2 oxidized in air or Ar/O_2 mixtures with an oxygen partial pressure of 0.2. Their data are compared with the model predictions in Fig. 4b and c. Again, the correspondence is taken to be quite reasonable given the assumed geometrical factors.

4.2. HfB_2

The model is easily extended to other diborides by simply using the appropriate thermodynamic data and the appropriate physical properties such as molecular weight,

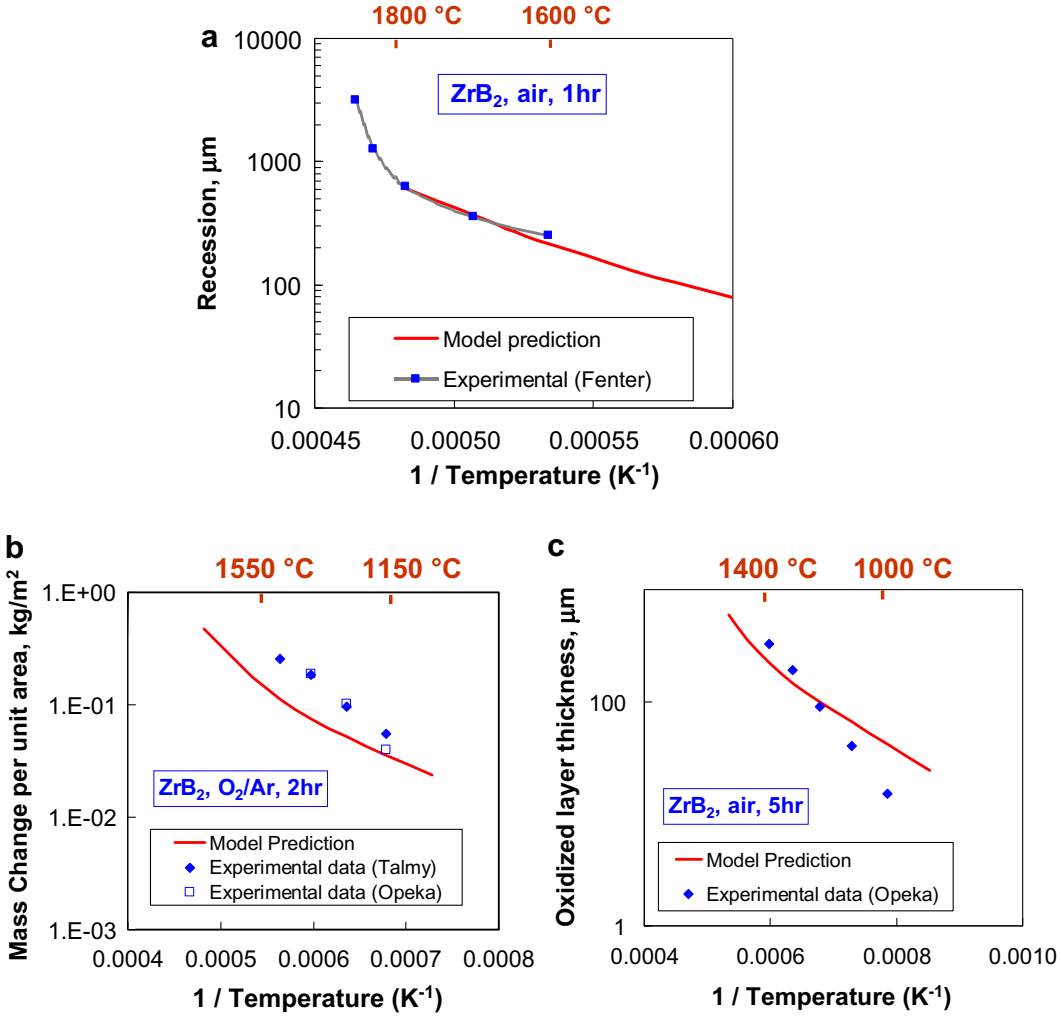

Fig. 4. (a) Model predictions of the recession in air as a function of temperature is shown compared with data of Kaufman and Clougherty [7,8] and Fenter [9]. (b) The model predictions for mass change are shown compared to experimental data obtained in Ar/O_2 gas in 2 h [10]. (c) The scale thickness obtained after 5 h in air by Opeka et al. is shown compared to the predictions. The porosity in the scale, f, was taken to be 0.05 and the pore radius to be 0.5 μm.

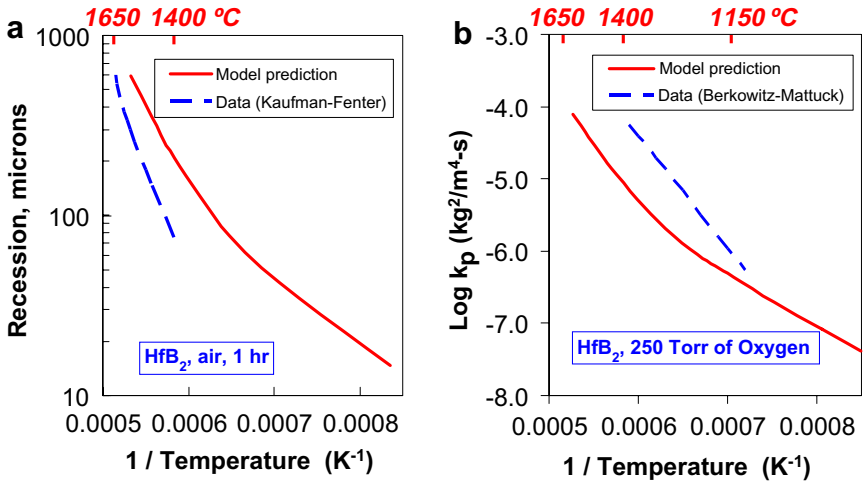

Fig. 5. Comparison of model predictions with experimental data on oxidation of HfB_2. (a) Recession in flowing air from Kaufman and Clougherty [7,8] and Fenter [9]. (b) Parabolic rate constant for weight gain as a function of temperature from Berkowitz-Mattuck in 250 Torr of oxygen [13]. The porosity in the scale, f, was taken to be 0.05 and pore radius to be 0.5 μm.

density, etc. For HfB_2, one obtains the oxygen partial pressure, $P^{s}_{O_2}$, at the HfB_2–B_2O_3 interface as:

$$P^{s}_{O_2}(HfB_2)\ (atm) = 6 \times 10^{9} \exp\left(-\frac{100,070}{T}\right). \quad (23)$$

Two reports in the literature have characterized the oxidation behavior of HfB_2. Fenter [9] summarized the measured recession rates in flowing air, while Berkowitz-Mattuck [13] reported on the parabolic rate constants in 250 Torr of pure oxygen. These data are compared with the model predictions using a pore fraction of 0.05 and pore radius of 0.5 μm in Fig. 5. The predicted recession is higher than the measured values, while the predicted parabolic rate constants are lower.

4.3. TiB_2

For TiB_2, one obtains the oxygen activity, $P^{s}_{O_2}$, at the TiB_2–B_2O_3 interface as:

$$P^{s}_{O_2}(TiB_2)\ (atm) = 5 \times 10^{10} \exp\left(-\frac{95,126}{T}\right). \quad (24)$$

By use of the appropriate physical properties for TiO_2 and TiB_2 the oxidation behavior was predicted, once again assuming a pore fraction of 0.05 and a pore radius of 0.5 μm. The predictions were evaluated by comparing with experimental data available on weight change and recession reported by Koh et al. [25]. This comparison is shown in Fig. 6.

5. Parametric/sensitivity studies

A parametric study was conducted to assess model sensitivity and to determine the effects of experimental variables. Fig. 7 shows the temperature dependence of the parabolic rate constant for oxidation of ZrB_2. A clear

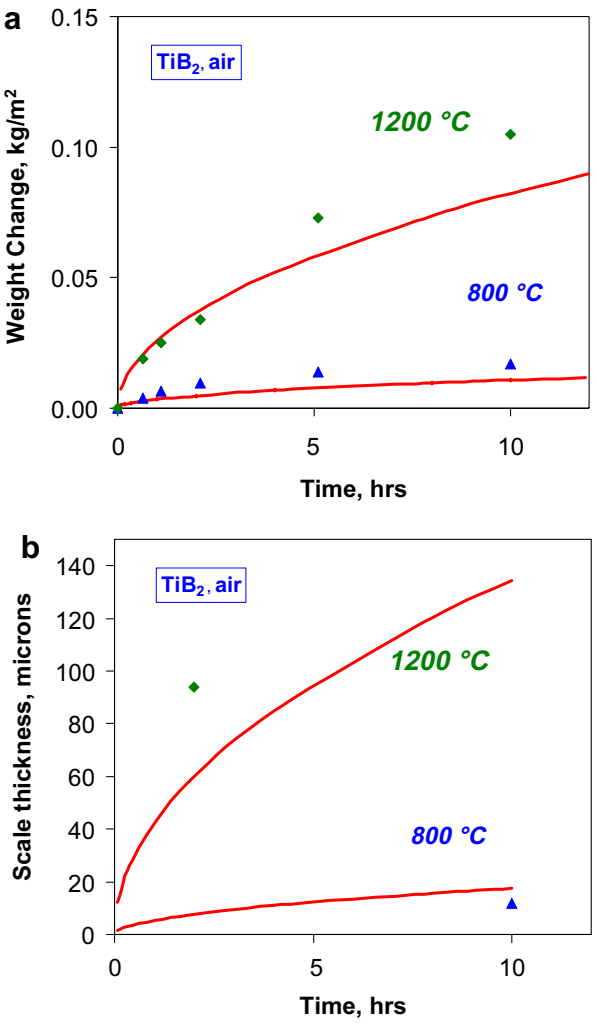

Fig. 6. Comparison of model predictions with experimental data on TiB_2. (a) Weight gain with time in air and (b) scale thickness after oxidation in air. The porosity in the scale, f, was taken to be 0.05, with a pore radius of 0.5 μm. The data were obtained from Koh et al. [25].

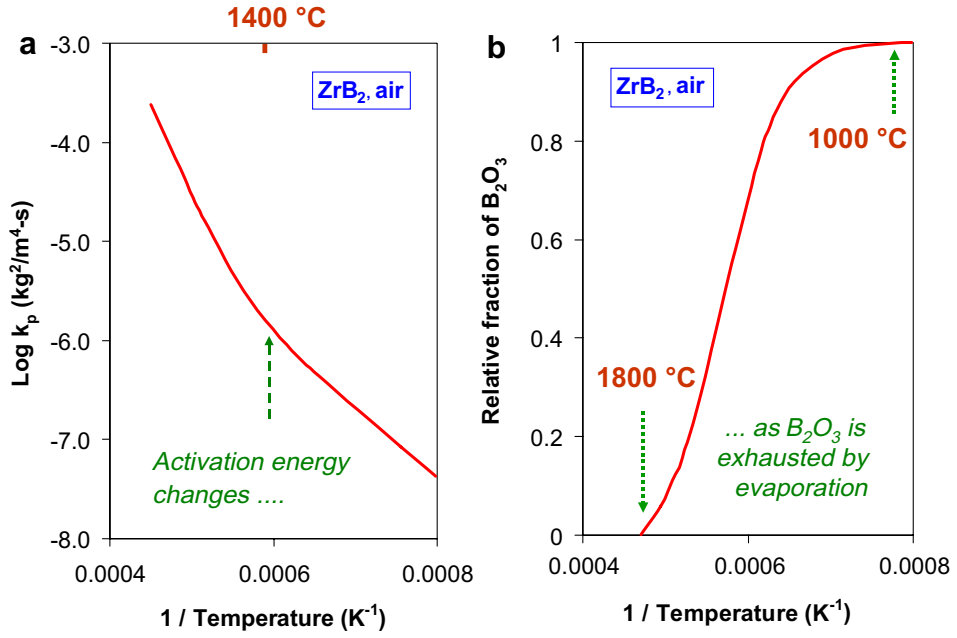

Fig. 7. Results of a parameteric study on the effect of temperature on oxidation behavior of ZrB_2. (a) The parabolic rate constant and (b) the relative fraction of liquid boria in the scale. The model predicts a change in the apparent activation energy for the parabolic rate constant that correlates with loss of boria from the scale.

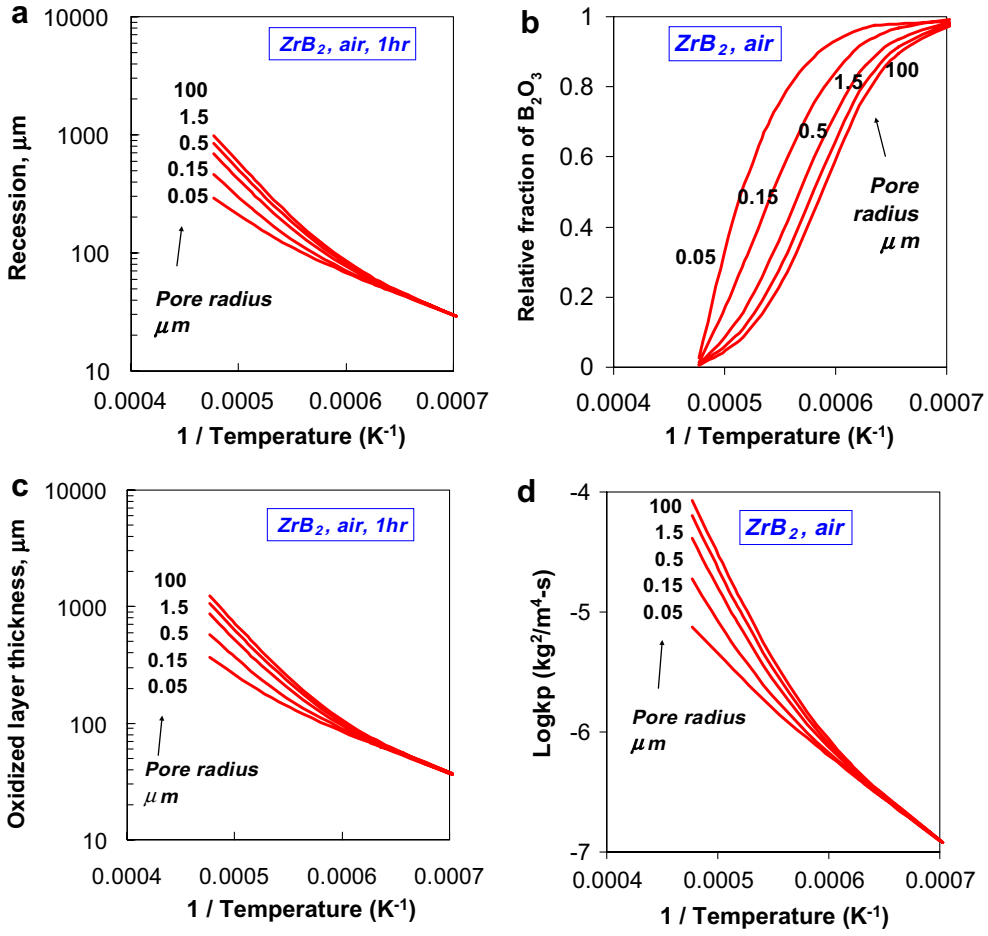

Fig. 8. The effect of pore radius (Knudsen effect) on: (a) recession, (b) boria fraction in scale, (c) oxide thickness and (d) parabolic rate constant.

change in apparent activation energy is seen at around 1400 °C. The figure includes the predicted fraction of boria (h/L) in the scale. The change in activation energy clearly arises from the loss of boria from the scale.

Next, the model was used to study the effect of varying the pore fraction and pore radius, to assess its sensitivity. These parameters are difficult to measure and have not been reported experimentally. Further, since the model neglects the tortuosity of the porous scale, the pore radius and pore fraction used in the model must be considered to be "effective" parameters rather than the actual physical values. It is quite possible that these parameters themselves vary with temperature or other experimental conditions such as environment. Thus it is useful to conduct a sensitivity study.

Fig. 8 shows the effect of pore radius on the recession, scale thickness, parabolic rate constant, and the thickness fraction of boria in the scale. The choice of pore radius is significant when the pore radius is smaller than about 1 μm. However, the effect is insignificant at temperatures below about 1400 °C, which corresponds to the temperature at which boria evaporation becomes significant.

Fig. 9 shows the effect of pore fraction on the oxidation behavior of ZrB_2 in air. The rate constant, scale thickness and recession all increase by about an order of magnitude when the pore fraction is increased from 0.025 to 0.2. Thus the effect is nearly linear.

Comparing Figs. 8 and 9 to Figs. 3–5 it can be seen that very close correspondence between the model and experimental data could be obtained if pore fraction and/or pore radius are taken to vary rather than remain constant for all scales. The scatter in the experimental results alone implies that these geometrical parameters may vary depending on the exposure temperature, and/or experimental conditions such as flow rates of gases, and humidity, and they may even change somewhat during the course of an experiment. The literature data is typically incomplete with respect to details of the environment, especially humidity, and the scale microstructures.

Fig. 10a summarizes the effect of oxygen partial pressure in O_2/N_2 gas mixture of 1 atm total pressure, on the parabolic rate constant as a function of temperature. The dependence is linear at 1000 °C and becomes negligible at

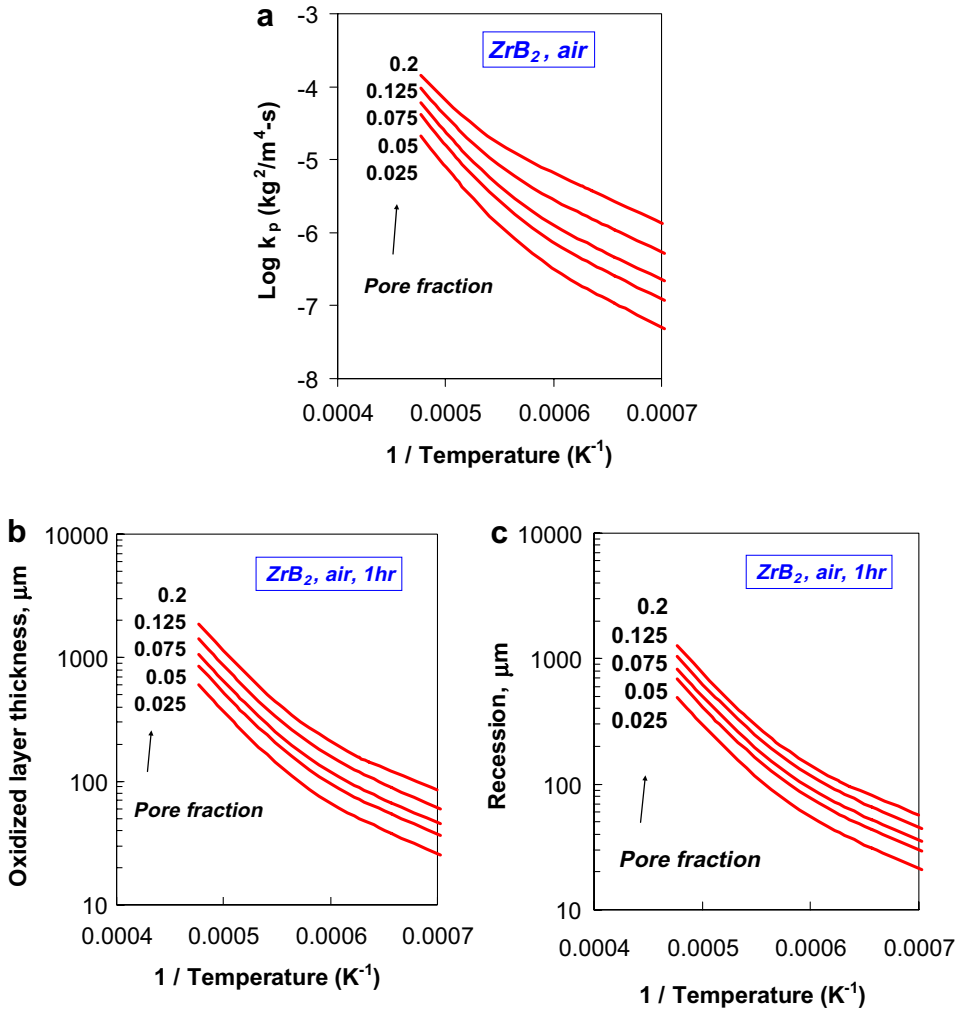

Fig. 9. The effect of pore fraction on: (a) rate constant, (b) oxide thickness and (c) recession, for a change in pore fraction from 0.025 to 0.2.

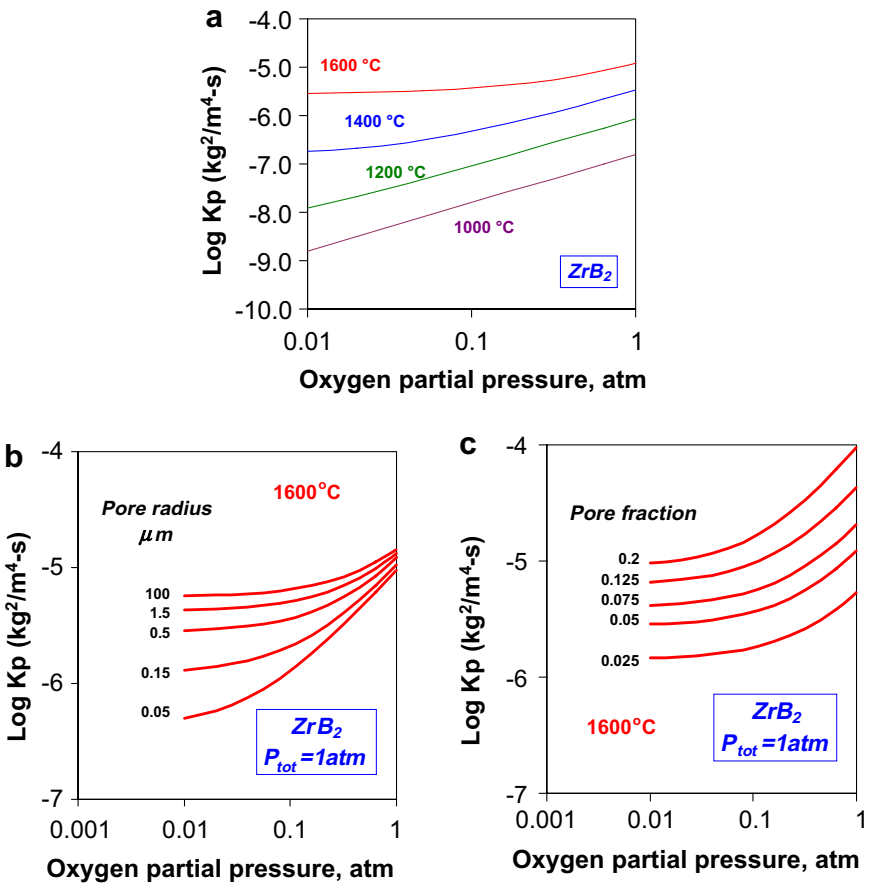

Fig. 10. Parametric studies of the dependence of: (a) parabolic rate constant on the oxygen partial pressure in O_2/N_2 gas mixture (1 atm total pressure). The P_{O_2} dependence itself is dependent on (b) the pore size and (c) pore fraction.

1600 °C; this is consistent with the experimental observations of Berkowiz-Mattuck [13]. Fig. 10b shows that the pore radius is predicted to have a significant effect at low oxygen partial pressures and the pore fraction has a near-linear effect (Fig. 10c) as might be expected.

6. Summary

A physical model to predict the oxidation behavior of refractory diborides in the intermediate temperature regime (1000–1800 °C) is presented. The model assumes that the refractory oxide product does not support significant oxygen diffusion due to a low oxygen vacancy concentration and to a lack of sufficient electronic conductivity. The porosity in the base of the oxide is assumed to be filled with liquid boria which, however, evaporates from the surface. A comparison of the model with experimental data in the literature shows reasonable agreement in predicting weight change, metal recession, oxide scale thickness and the temperature dependence of the parabolic rate constant for ZrB_2, even with postulated values for pore geometry and unknown experimental flow rates. Comparison with limited literature data for HfB_2 and TiB_2 show that the model may have a general applicability to refractory diborides, although data on oxygen diffusion and electronic conductivity of the oxides, especially at high temperatures, will be required to refine the model.

Acknowledgements

It is a pleasure to acknowledge useful discussions with Dr. I. Talmy of Naval Surface Warfare Center, Carderock Division, West Bethesda, MD, who shared some of her unpublished work. We acknowledge discussions with all the participants of a workshop on UHTC, sponsored by Dr. Joan Fuller of the Air Force Office of Scientific Research (AFOSR) in 2005. This work was supported in part by USAF Contract No. FA8650-04-D-5233.

Appendix. Discounting ambipolar oxygen diffusion in zirconia

In the model for refractory diboride oxidation, the diffusion of oxygen, via ambipolar diffusion, is considered to be negligible because of the low magnitudes of oxygen vacancies and p-type electronic conduction in the zirconia oxidation product. In the relatively high oxygen activities encountered in the oxidation, only p-type electronic con-

duction needs to be considered; n-type conduction is negligible. In fact, data are not available for the magnitude of the p-type electronic conductivity in relatively pure ZrO_2, but some measurements have been made for calcia-stabilized-zirconia, e.g. $Zr_{0.85}Ca_{0.15}O_{1.85}$, as a function of temperature. The interpretation of defect equilibria by Lasker and Rapp [26] permits a general evaluation of p-type conductivity as a function of dopant concentration and oxygen activity to provide magnitudes for the ionic and p-type electronic conductivities for compositions with much lower dopant concentrations.

Consider the defect equilibrium for zirconia:

$$O_O^x + 2\dot{h} \Longleftrightarrow \frac{1}{2}O_2\ (g) + V_{\ddot{O}}, \tag{A1}$$

where O_O^x is an oxygen ion on an oxygen lattice site, $V_{\ddot{O}}$ is a doubly ionized oxygen vacancy and $\dot{h}$ is a positive hole. From the law of mass action:

$$K_{A1} = \frac{[V_{\ddot{O}}]P_{O_2}^{1/2}}{[\dot{h}]^2}. \tag{A2}$$

If the zirconia were doped by substitution of an aliovalent solute, e.g. Ca^{2+} ions, on the Zr^{4+} lattice sites, then the simplified electrical neutrality condition would read:

$$2[Ca''_{Zr}] = 2[V_{\ddot{O}}] \ll [\dot{h}]. \tag{A3}$$

Upon substitution of Eq. (A3) into Eq. (A2), two predictions arise:

$$[V_{\ddot{O}}] \propto [Ca''_{Zr}] \neq f(P_{O_2}) \tag{A4a}$$

$$[\dot{h}] \propto [Ca''_{Zr}]^{1/2}(P_{O_2})^{1/4}. \tag{A4b}$$

From the usual justified assumption of concentration-independent mobilities of the oxide ions and positive holes, the ionic conductivity and p-type electronic conductivity obey the same dependencies as Eqs. (A4a) and (A4b).

Patterson [27] has presented an evaluation of the ionic transference number for $Zr_{0.85}Ca_{0.15}O_{1.85}$ (CSZ) as a function of temperature to establish the electrolytic domain. From a knowledge of the ionic conductivity, provided by Patterson et al. [28] and Patterson's transference numbers [27], the p-type electronic conductivity for CSZ can be calculated. Then, using Eqs. (A4a) and (A4b), the functions can be applied to nearly pure ZrO_2, e.g. containing 150 ppm divalent impurity concentration.

From Patterson et al. [28] for 0.15CaO-stabilized ZrO_2 (CSZ), using the ionic conductivity at 1273 K and the reported activation energy, the oxygen partial pressure-independent ionic conductivity is given as:

$$\sigma_{ion}\ (\Omega^{-1}\ cm^{-1}) = 2323 \exp\left(-\frac{123,500}{8.314T}\right). \tag{A5}$$

Similarly, the p-type electronic conductivity in CSZ can be derived. The reported hole conductivity is $2 \times 10^{-4}\ \Omega^{-1}\ cm^{-1}$ at 1273 K and $P_{O_2} = 10^6$ with $t_{ion} = 0.99$. Further, the ionic conductivity equals the hole conductivity at $(1/T,\ P_{O_2})$ values of $(0.0003,\ 10^3)$ and $(0.0012,\ 10^{24})$. From these data, and combining with Eq. (A5), for conditions where $\sigma_{ion} = \sigma_{\dot{h}}$, the hole conductivity is obtained as:

$$\sigma_{\dot{h}}\ (\Omega^{-1}\ cm^{-1}) = 23,280 P_{O_2}^{1/4} \exp\left(-\frac{235,200}{8.314T}\right). \tag{A6}$$

From Lasker and Rapp [26], the dependence on [Ca] is given as:

$$\sigma_{\dot{h}} \propto [Ca''_{Zr}]^{1/2}, \quad \sigma_{ion} \propto [Ca''_{Zr}]^{1}. \tag{A7}$$

Combining Eqs. A5, A6, A7 one obtains:

$$\sigma_{ion}\ (\Omega^{-1}\ cm^{-1}) = \frac{[C_{dopant}]}{0.15} 2323 \exp\left(-\frac{123,500}{8.314T}\right); \tag{A8}$$

$$\sigma_{\dot{h}}\ (\Omega^{-1}\ cm^{-1}) = \left(\frac{[C_{dopant}]}{0.15}\right)^{1/2} 23,280 P_{O_2}^{1/4} \exp\left(-\frac{235,200}{8.314T}\right). \tag{A9}$$

Consider a ZrO_2 composition doped with 150 ppm of a divalent impurity. At 1273 K, the ionic and hole conductivities are $2 \times 10^{-5}\ \Omega^{-1}\ cm^{-1}$ and $1.64 \times 10^{-7}\ \Omega^{-1}\ cm^{-1}$, respectively, with a transference number $t_{ion} = 0.9918$. Thus the assumption of negligible ambipolar diffusion is validated for this temperature.

At 1873 K, the ionic and hole conductivities are $8.35 \times 10^{-4}\ \Omega^{-1}\ cm^{-1}$ and $2.03 \times 10^{-4}\ \Omega^{-1}\ cm^{-1}$, respectively, with a transference number $t_{ion} = 0.804$. Thus, at these higher temperatures, p-type conductivity becomes more important and ambipolar diffusion of oxide ions cannot be neglected. However, at high temperatures, the pores in the zirconia are expected to be devoid of the boria glass due to evaporation. Thus it is unlikely that ambipolar oxygen diffusion could contribute a flux that is competitive with respect to gaseous diffusion of oxygen molecules in the gas phase. The assumption of at least 150 ppm of aliovalent impurity in the zirconia oxidation product is not unrealistic. The remaining issue with this analysis is the assumption that the lightly doped zirconia product would exist in a CaF_2-type lattice structure for the scale; however, if the zirconia scale existed on a different crystalline state (e.g. tetragonal or monoclinic), the oxygen diffusivity would certainly be negligible regardless of the electronic conductivity.

References

[1] Savino R, Fumo MDS, Paterna D, Serpico M. Aerothermodynamic study of UHTC-based thermal protection systems. Aerospace Sci Tech 2005;9:151–60.

[2] Boyd ID, Padilla JF. Simulation of sharp leading edge aerothermodynamics. AIAA 2003;1–10:2003–7062.

[3] Opeka MM, Talmy IG, Zaykoski JA. Oxidation-based materials selection for 2000 °C + hypersonic aerosurfaces: theoretical considerations and historical experience. J Mater Sci 2004;39:5887–904.

[4] Wuchina E, Opeka M, Causey S, Buesking K, Spain J, Cull A, Routbort J, Guitierrez-Mora F. Designing for ultrahigh-temperature applications: The mechanical and thermal properties of HfB_2, HfC_x, HfN_x and a-Hf(N). J Mater Sci 2004;39:5939–49.

[5] Tului M, Marino G, Valente T. Plasma spray deposition of ultra high temperature ceramics. Surf Coat Technol 2006;201(5):2103–8.

[6] Wank A, Wielage B, Podlesak H, Matthes KJ, Kolbe G. Protection of Ti6Al4V surfaces by laser dispersion of diborides. J Thermal Spray Tech 2005;14(1):134–40.
[7] Kaufman L, Clougherty E. Technical Report RTD-TDR-63-4096: Part 1, AFML, WPAFB, OH; 1963.
[8] Kaufman L, Clougherty E. Technical Report RTD-TDR-63-4096: Part 2, AFML, WPAFB, OH; 1965.
[9] Fenter JR. Refractory diborides as engineering materials. SAMPE Quarterly 1971;2(3):1–15.
[10] Opeka MM, Talmy IG, Wuchina EJ, Zaykoski JA, Causey SJ. Mechanical, thermal and oxidation properties of refractory hafnium and zirconium compounds. J Eur Ceram Soc 1999;19:2405–14.
[11] Levine SR, Opila EJ, Halbig MC, Kiser JD, Singh M, Salem JA. Evaluation of ultra-high temperature ceramics for aeropropulsion use. J Eur Ceram Soc 2002;22:2757–67.
[12] Fahrenholtz WG. The ZrB2 volatility diagram. J Amer Ceram Soc 2005;88(12):3509–12.
[13] Berkowitz-Mattuck JB. J Electrochem Soc 1966;113:908.
[14] Barin I. Thermochemical data of pure substances. New York: VCH Verlagsgesellschaft; 1995.
[15] Tokuda T, Ido T, Yamaguchi T. Z Natuforschung 1971;26A:2058–60.
[16] Courtright EL. Engineering property limitations of structural ceramics and ceramic composites above 1600C. Ceram Eng, Sci Proc 1991;12(9–10):1725–44.
[17] Luthra KL. Oxidation of carbon/carbon composites – a theoretical analysis. Carbon 1988;26:217–24.
[18] Welty JR, Wicks CE, Wilson RE. Fundamentals of momentum, heat, and mass transfer. New York: John Wiley; 1984.
[19] Bird RB, Stewart WE, Lightfoot EN. Transport phenomena. New York: John Wiley; 2002.
[20] Svehla RA. Estimated viscosities and thermal conductivities of gases at high temperatures. NASA Tech report R-132; 1962.
[21] Szekely J, Evans JW, Sohn HY. Gas solid reactions. New York: Academic Press; 1976.
[22] Tripp WC, Graham HC. Thermogravimetric study of the oxidation of ZrB2 in the temperature range of 800 to 1500 °C. J Electrochem Soc 1971;118(7):195–1199.
[23] Kuriakose AK, Margrave JL. J Electrochem Soc 1964;111:827.
[24] Talmy I, Zaykoski J, Opeka M, Smith A. Oxidation of ZrB_2 ceramics containing Si_3N_4. Personal communication of unpublished work; 2005.
[25] Koh Y-H, Lee S-Y, Kim H-E. Oxidation behavior of titanium boride at elevated temperatures. J Amer Ceram Soc 2001;54(1): 229–41.
[26] Lasker MF, Rapp RA. Z Phys Chem Neue Fol 1966;49:198–221.
[27] Patterson JW. J Electrochem Soc 1971;118:1033–9.
[28] Patterson JW, Bogren EC, Rapp RA. J Electrochem Soc 1967;114: 752–8.